https://doi.org/10.48048/tis.2023.6626

Magnetic Properties of Ancient Sediments Bengawan Solo, Central Java-East Java, Indonesia

Budi Legowo[1,*], Shandiyano Putra[1], Heri Purwanto[1], Hamdi Rifai[2], Wiwit Suryanto[3] and Budi Purnama[1]

[1]Department of Physics, Sebelas Maret University, Jawa Tengah 57126, Indonesia
[2]Department of Physics, Padang State University, Padang 25131, Indonesia
[3]Department of Physics, Gadjah Mada University, Yogyakarta 55281, Indonesia

([*]Corresponding author's e-mail: pakbeel@staff.uns.ac.id)

Received: 15 January 2023, Revised: 11 February 2023, Accepted: 15 February 2023, Published: 10 March 2023

Abstract

Information about the eruption of Mount Lawu in Central Java Province in 1885 and Mount Merapi in D.I. Yogyakarta in 2010 became a source for estimating the presence of magnetic minerals which underwent a sedimentation process in the Bengawan Solo River from upstream (Wonogiri) - downstream (Bojonegoro). The results we get of the magnetic susceptibility distribution of the Bengawan Solo sediments reveal that the sediment from the upper reaches of the Bengawan Solo River has a low frequency magnetic susceptibility value in upstream of around $1{,}080.23\times10^{-8}$ m^3/Kg - $2{,}780.77\times10^{-8}$ m^3/Kg, the middle part is 74.40×10^{-8} m^3/Kg - $1{,}735.90\times10^{-8}$ m^3/Kg, and downstream 17.57×10^{-8} m^3/Kg - $1{,}620.53\times10^{-8}$ m^3/Kg. The value of magnetic susceptibility decreased significantly from upstream to downstream. High susceptibility indicates the sample contains metal elements. In determining iron oxide, we use X-Ray Fluorescence assisted by X-Ray Diffractometer testing to determine magnetic minerals. X-Ray Fluorescence confirm metal oxide in the sample. There are Al and Fe confirm the presence of magnetic properties in sedimentation. The Vibrating Sample Magnetometer confirmed that the Bengawan Solo sediment has a magnetic saturation about 0.06 - 9.50 (emu/g), a magnetic remanent around 0.001 - 0.575 (emu/g) and coercivity field of around 10 - 60.15 (Oe). X-Ray Diffractometer pattern confirm the mineral structures, namely Coesite, Magnetite, Cristobalite, Portlandite, Quartz, Anatase, Goethite, Tridymite, Gibsyte, Stishovite, Grasullaria, Labradorite and Wuestite. These results indicate the novelty of sediments from Bengawan Solo, Central Java to East Java.

Keywords: Bengawan solo, Miocene, Holocene, Sediment, Magnetic properties

Introduction

Bengawan Solo is the longest river on the island of Java, which is around 600 km. The upstream of the river originates from 2 places, namely around Mount Merapi and the South Mountains (Wonogiri). The two of them then met with the Madiun River in Ngawi, whose headwaters were located on the western slope of Mount Wilis. In the Ujungpangkah (Gresik) area of the Bengawan Solo empties into the Java Sea, the Bengawan Solo found many Quaternary sediment deposits [1].

Sediment is a fraction of mineral or organic material that undergoes a process of transportation from various sources and is deposited by the medium. Sediments found in rivers contain a variety of different minerals depending on the source of the deposited media. According to [2], rivers become a collection of minerals that can be analyzed, dust deposition from the atmosphere (volcanic ash), and minerals formed through authigenic processes. Research conducted by [3], it was confirmed that the magnetic values in the sediment ranged from 844 - $7{,}231.4\times10^{-8}$ m^3/Kg, this value was due to volcanic factors as metal oxide deposits in the surrounding area.

At this time the study of magnetic properties has been used in the field of advanced materials. Usually, they use magnetic susceptibility to get good materials. Good material with high susceptibility. The advanced materials that are being carried out in this era are [4-7]. Study of sediments in the Surabaya River [8], The magnetic susceptibility was obtained between 259.4 - $1{,}134.8\times10^{-8}$ m3/Kg. The PSD to MD domains dominates the minerals in the river environment, a grain size of 6 - 14 μm. The study [9], before being polluted by waste, the xlf magnetic susceptibility value was around $1{,}763.50\times10^{-8}$ m3/Kg, but after

being polluted by waste it changed to $1{,}907.33\times10^{-8}$ m3/Kg. It is ensured that the value from upstream to downstream has increased. The study [10], studies on yellow river sediments in the china area regarding magnetic properties as an indicator of heavy metals with the results of the most dominant elements being Co, Cr, Ni, Cu, Zn, and Pb. Studies conducted in the southern part of China on evidence of clay minerals and magnetic properties confirm that the minerals present in the study area are dominated by Magnetite, hematite and goethite on the sediment surface [11]. Studies conducted on the southern Tibetan Plateau regarding magnetic properties confirm that it is dominated by coarse ferrimagnetic grains [12]. Grain size-dependent studies on the magnetic properties of the Holocene delta sediments found that the mean grain size was < 16 um [13].

The emergence of the Bengawan Solo does not rule out the possibility of a fault. Based on the geological map, there are 4 types of faults, namely anticline faults [14], syncline faults [14,15], inactive faults [17], and inactive reverse faults [18]. In the middle of the Bengawan Solo there is an inactive reverse fault. The inactive reverse fault resulted in the central area appearing earlier than other areas of the Bengawan Solo. This is supported by the discovery of fossils in the Trinil area [19-22]. The central area of Bengawan Solo is the oldest among the other regions. The area is Miocene in age. The Miocene geological age scale is approximately 23.03 - 5.332 million years ago.

The Upper and Lower parts appear with the same geological age scale, namely the Holocene. The Holocene is a geological scale that is young among the Miocene geological scales. Meanwhile, the Mount Lawu area appears in the Holocene time span. This means that the initial hypothesis can be taken that the upstream and downstream are the result of the deposits of Mount Lawu and Mount Merapi. Researchers have recorded that the last eruption occurred on November 28, 1885 [23]. Volcanic material from the eruption of Mount Lawu spread in all directions [24]. Volcanic material resulting from the eruption has main elements in the form of Si, Al, and Ca and contains metal elements in the form of Fe, Pb, and Ti [25-28]. Elements contained in volcanic materials such as Fe are the constituent elements of magnetic minerals [29]. Mount Merapi's biggest eruption was recorded for the first time in 1548 [30].

Wind is a medium of transportation for Mount Lawu material, some sedimentation occurs around the mountain, some is carried by air to move from 1 place to another. As long as peace will be [31]. One of the possible places for the deposition of volcanic material is river sediments. The river that allows and is located around the Mountain area is Bengawan Solo. The purpose of this study is to see the magnetic properties of the Bengawan Solo because it is surrounded by volcanic eruptions.

Geologycal setting

Java island has the longest river, namely Bengawan Solo, about ~600 km^2. Bengawan Solo stretches from the Wonogiri area of Central Java Province as the upstream and ends in the Gresik area of East Java Province as the downstream [32]. The geology of Bengawan Solo is shown in **Figure 1**. In **Figure 1** we can see Bengawan Solo River starts from the Wonogiri area, East Java Province and reaches the Bojonegoro area on the eastern side of Surakarta City. Bengawan Solo is formed from several formations and the influence of Lahar from Mount Lawu. The South Side of Surakarta City is dominated by Alluvial. Alluvial form of sediment along the south side to Surakarta City. The southern side of Surakarta City, precisely the Wonogiri area, is confirmed from the geological map in **Figure 1** to have a Holocene age. The age of the Holocene on a geological scale range from $11{,}430 \pm 130$ years ago.

Continued with the eastern side of Surakarta City formed from alluvial which is confirmed to be the same as the southern area of Surakarta City with the same age. On the North side it is dominated by 3 formations forming the Bengawan Solo River. The 3 formations are the Tambakrumo Formation, the Pucangan Formation, and the Kalibeng Formation. Based on the geological scale and geological map in **Figure 1**, the 3 formations were formed at different times from 1 another [33]. The first formation was the Kalibeng formation. The Kalibeng Formation was formed around 23.03 - 5.332 mya. Followed by the formation of the Pliocene Pucangan Formation. It is confirmed that the age of the Pliocene was formed around 5,332 to 1,806 million years ago. The last formation formed on the north side of Surakarta City is Tambakrumo. The Tambakrumo Formation is confirmed to have formed on the Pleistocene geological scale. The Pleistocene geological scale has confirmed an age of around 2.58-million years to 11,500-thousand years ago.

Almost all formations are dominated by sediments. The sediments are either coarse or fine textured. This is due to erosion and weathering factors in an area. The high erosion rate results in the complete change of coarse materials into fine grains [34,35]. Inversely proportional to areas that have low erosion rates. Materials with large sizes and rough textures cannot be completely transformed. The level of weathering also has an impact on the texture of the materials found at the location. The same applies to areas that have

high or low erosion rates. Usually, areas that have a high level of weathering are dominated by active and numerous microbes. These microbes cause materials to change shape from coarse to fine grains [36].

In addition to the formations that were formed in the Bengawan Solo area, there are faults that make the Bengawan Solo area appear to the surface. There are 4 types of faults in the Bengawan Solo area confirmed. These faults are Anticlinal Faults, Cycline Faults. Inactive fault, and inactive reverse faults.

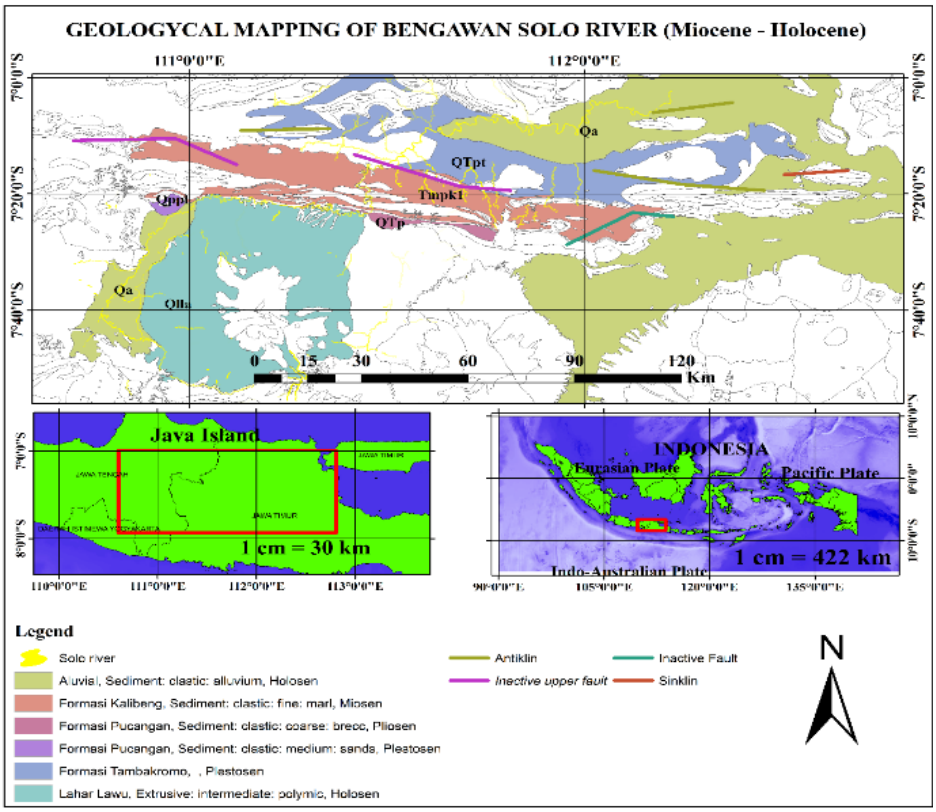

Figure 1 geological map of Bengawan Solo which stretches from Central Java Province to East Java. In the formation of Bengawan Solo, there are 6 formations that form the basis for the formation of Bengawan Solo sediments. Apart from the formations mentioned.

Materials and methods

We do this study on a stretch of geographic position. The Bengawan Solo area is divided into 3 parts, namely Upstream, Middle, and Downstream. The upper part starts from E110.926 - S7.826, the middle E111.224 - S7.365 and the lower part E111.438 - S7.273 can be seen in **Figure 3**. From all sides only in the middle part were found ancient heritage sites. The site is Trinil. As explained in the introductory section, the researchers had already found ancient relics in the Trinil area. As an initial indication that the discovery, and confirmation of **Figure 1**, it is true that the middle section is the oldest site compared to the other 2 s. In this study, we focus on upstream sites starting from the Wonogiri area to the downstream ending in the Bojonegoro area. Upstream to downstream is ~200 km^2. The distance between 1 sample and another is ~13 km^2. From all sections we took 23 samples for magnetic susceptibility testing while for the X-Ray Diffractometer, X-Ray Fluoresence and Vibrating Sample Magnetometer tests we analyzed 15 samples from 28 samples. This is due to the formation factors involved in the formation of the Bengawan Solo River. Therefore, the raw sample is washed to obtain pure sediment. We wash using aquadest. After the samples were washed, they were dried in a memmert oven at 100 °C for 12 h. We use Bartington Magnetic Susceptibility as an instrument in measuring the magnetic value of materials with sensor B (MS2B) (Bartington Instrument Ltd., Whitney, UK) which operates at 2 frequencies, namely 470 Hz (low frequency xlf) and 4,700 Hz (high frequency xhf). We used a Vibrating Sample Magnetometer (VSM) (Type: Versa Lab, Quantum design) test at room temperature to obtain the saturation magnetization (Ms), remanent magnetization, and coercivity field (Hc). In determining the metal oxide in the sample, we used X-Ray Fluorescence brand: PANalytical, Type: Manipal 4. Mineral analysis in sediments using X-Ray Diffractometer with Cu K radiation, used 10 - 90 °.

(a) (b)

Figure 2 Several locations of the Bengawan Solo River are in the middle and downstream. (a) middle Section (SR 9); (b) Downstream section we found outcrop (SR 14).

Table 1 Description of samples taken in the field.

Code	Coordinates	Description
SR 1	110.926 E; 7.826 S	The sample is sedimentation. Fine grain shape. Size is about 1 - 5 mm. blackish brown in color.
SR 2	110.936 E; 7.781 S	
SR 3	110.824 E; 7.726 S	
SR 4	110.800 E; 7.634 S	
SR 5	110.843 E; 7.580 S	
SR 6	110.893 E; 7.510 S	
SR 7	110.961 E; 7.394 S	
SR 8	111.224 E; 7.365 S	Samples were taken from sedimentation that had long settled. approximately. 1 - 6 mm. Fine grain shape.
SR 9	111.358 E; 7.375 S	The sample is sedimentation. Yellowish brown in color. The sample is in the form of coarse grains measuring 1 - 6 cm.
SR10	111.452 E; 7.390 S	The sample is in the form of pebbles measuring 1 - 3 cm. blackish brown in color. Possibly as a breeding ground for living things in ancient times.
SR11	111.438 E; 7.273 S	The sample is in the form of fine gravel measuring 1 - 5 mm. blackish brown.
SR12	111.598 E; 7.154 S	Samples were taken in the middle of the Bengawan Solo River. In the form of coarse gravel measuring 1 - 3 cm
SR13	111.726 E; 7.115 S	Samples were taken from the sedimentation process. Blackish yellow. Fine grain size of 1 - 7 mm.
SR14	111.896 E; 7.136 S	The sample is an outcrop that is still fresh. Brownish yellow in color. In the form of fine gravel.
SR15	111.040 E; 7.342 S	The sample is an outcrop that has become rocks. As a place to live for ancient living things.

Results and discussion

Magnetic susceptibility (MS2B)

The results obtained from the Barthington Susceptibility Meter Sensor B test can be seen in **Table 2** and from these values a mapping can be made according to **Figure 3**.

Table 2 The value of magnetic susceptibility from upstream to downstream.

Code	Average $(\chi_{lf})(10^{-8}$ m^3/Kg)	Average $(\chi_{hf})(10^{-8}$ m^3/Kg)
SR 1	2,780.77	2,766.47
SR 2	1,490.9	1,472.5
SR 3	2,544.83	2,521.83
SR 4	1,080.23	1,076.3
SR 5	2,007.6	2,001.83
SR 6	2,392.07	2,382.13
SR 7	1,586.2	1,582.33
SR 8	803.27	794.97
SR 9	969.7	961.07
SR 10	1,735.9	1,730.4
SR 11	1,035.73	1,032.67
SR 12	1,620.53	1,614.73
SR 13	505.93	503.9
SR 14	17.57	17.33
SR 15	74.4	74.33
R1	3,745.1	3,742.7
R2	3,891	3,842
R3	3,632.7	3,599.7
R4	5,262.1	5,216.8
R5	2,939.2	2,938.4
R6	2,453.7	2,451.1
R7	1,467.5	1,467.1
R8	1,940.3	1,926.3
China [37]	7.645 ~ 11.87	7.466 ~ 11.76
Morocco [38]	53.80	-
Indonesia (South Sulawesi) [39]	47.7 - 968.7	45.7 - 957.4
Indonesia (West Sumatra) [40]	291.1 - 12,445.5	-
Vietnam [41]	48	26

Table 2 and **Figure 3** confirm that points R1-8 are points taken around Mount Lawu which have large magnetic susceptibility values. This is because the volcanic material containing metal oxide contained in the sample is very high. So, because of the presence of metal oxide, the measured sample has a high value as well [9]. It has a positive correlation with 1 another. In **Table 2** is divided into 2 different codes. The first part is SR1 - 15. The code is part of Bengawan Solo. While the second part, namely R1 - 8, is bomb material resulting from the eruption of Mount Lawu. Between the 2 parts it is confirmed that the second part is higher than the first part. However, the downstream and middle sections of the Bengawan Solo have

high values due to factors caused by the mixing of Mount Lawu eruption material with Bengawan Solo sediment material.

From **Figure 2** the susceptibility values generated by the Bengawan Solo samples varied greatly. From the point of collection location with the distance of Mount Lawu to the sampling point, Mount Lawu provides eruption material to the upstream part of the Bengawan Solo. Comfirm that in the western part of Mount Lawu is confirmed to be high compared to the northern part of the Bengawan Solo.

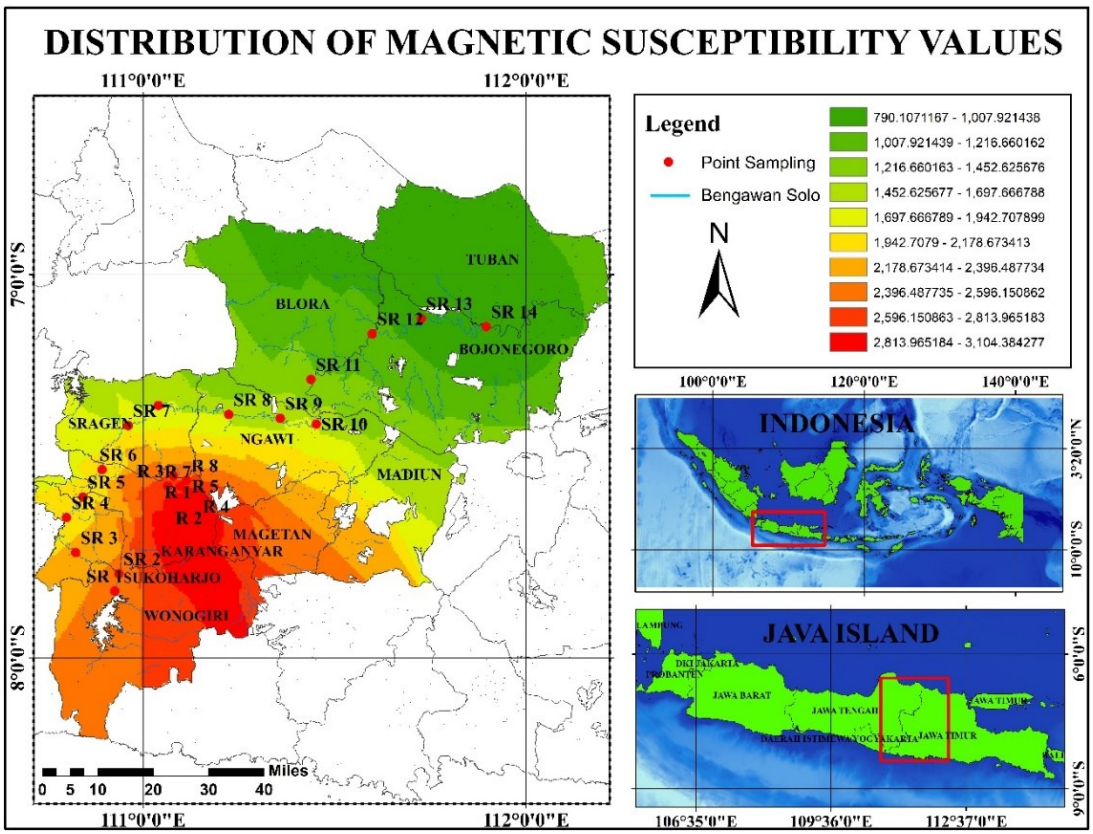

Figure 3 Distribution of magnetic susceptibility of Bengawan Solo River. The lower value of magnetic susceptibility is presented from upstream to downstream. Evidenced by the presence of significant color differences between the upstream and downstream.

Magnetic susceptibility is a value as an indication of the material containing magnetic minerals. Magnetic susceptibility is the ability of a material to accept an external magnetic field. High or low magnetic susceptibility as an indication that the presence of magnetic minerals in the material [42]. The high magnetic susceptibility value is also an indication that it is increasingly difficult for a material to accept an external magnetic field. So, the material is very good for doing research. Materials that contain Ferromagnetic properties have unique characteristics compared to Ferrimagnetic and Ferromagnetic. This characteristic is that if the magnetic field is removed or forced to touch zero, the ferromagnetic material still retains a magnetic remanent. This feature is utilized by researchers, especially in the paleomagnetic field.

The results of the eruption of Mount Lawu were deposited or there was a sedimentation process in the western (upstream) part of the Bengawan Solo. This deposit causes magnetic susceptibility value to increase. The northern part of the Bengawan Solo is confirmed to be low. Magnetic susceptibility values for the Middle and Downstream sections were found to be anomaly.

The anomaly at the middle SR 15 and downstream SR 14 points confirmed the lowest magnetic susceptibility values compared to the other sections. Point SR 14 obtained an outcrop. The outcrop consists of red clay. The outcrop contains poor magnetic minerals. The SR 15 point in the center is the same as the SR 14 point. An outcrop is found that has hardened into a rock. From the susceptibility value, it can be seen that the SR 14 point also contains quite a few magnetic minerals. So that it can be analyzed that the value of susceptibility decreases from upstream to downstream.

X-Ray fluorescence (XRF)

We get the elemental oxide concentration showed at **Table 3**. The identified ingredients are presented in **Table 3** where the concentration is in percent (%). From **Table 3** it is known that there are 20 oxide bonds.

There are 6 oxide bonds with dominating concentrations starting from the highest concentration, namely iron oxide (Fe-O), silica oxide (Si-O), aluminum oxide (Al-O), calcium oxide (Ca-O), thallium oxide (Ti-O), and potassium oxide (K-O) as well as 13 oxide bonds with concentrations below 1 %.

Table 3 The composition of elements in the Bengawan Solo samples from upstream to downstream.

Code	Oxide concentration (%)						
	Al-O	**Si-O**	**K-O**	**Ca-O**	**Ti-O**	**Fe-O**	**Others**
SR 1	12	29.4	1.1	9.51	2.47	43.13	2.39
SR 2	14	25.5	0.45	4.16	2.41	50.52	2.96
SR 3	10	27.2	0.8	5.51	3.59	49.58	3.32
SR 4	12	34.1	2.57	13.5	1.88	31.9	4.05
SR 5	11	28.7	1.5	11.3	3.02	41.3	3.18
SR 6	11	29	1.6	11.4	3.15	40.6	3.25
SR 7	11	28.7	1.66	11.2	3.06	40.86	3.52
SR 8	10	27.9	1.5	15.1	3.07	39.1	3.33
SR 9	10	30	1.3	18.5	2.58	34.5	3.12
SR 10	9.8	26.1	1.3	17.7	3.22	38.6	3.28
SR 11	11	27.6	1.3	12	3.23	42.62	2.25
SR 12	6.9	24.2	1.53	27.7	2.8	34.4	2.47
SR 13	8.7	28.8	1.3	22.8	2.59	33.3	2.51
SR 14	0	21.7	0.56	56.2	2.46	15.5	3.58
SR 15	1.2	3.7	0	80.74	0.73	8.98	4.65
Kosovo [43]	Fe > Mn > Zn > Sb > Ni > Sn > Cu > Rb > Pb > Cd > Ag						
Western United States [44]	Most Pb, As, Cu, and Cr						
Italy [45]	Most Cu, Pb, and Zn						

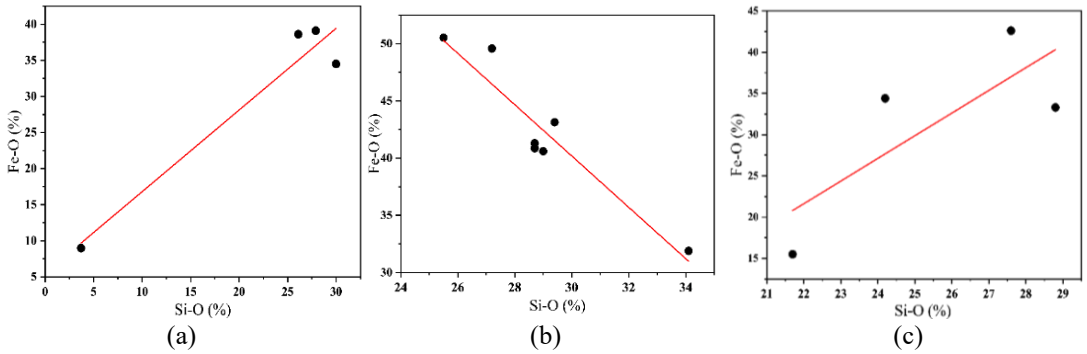

Figure 4 The relationship between metal oxide of Fe-O and Si-O Bengawan Solo River section, (a) upstream; (b) Downstream; (c) Middle.

The erosion process during the transportation stage of volcanic materials from Mount Lawu to the Bengawan Solo, one of the most dominant means of transportation, is water. Water sources can come from rainwater or river flow. The erosion rate is proportional to the intensity of the rains increases and the steepness of the slopes [46]. The largest river flowing material from the mouth of Mount Lawu is the Bengawan Solo River. The results of the XRF test in the Bengawan Solo section showed the dominant metal oxide is iron oxide (Fe-O) content because in the earth's crust the dominant element is Fe [47].

In **Figure 4(a)** graph of the relationship between Si-O and Fe-O where (a) is upstream; (b) middle part; and (c) downstream. From the 3 graphs it shows that there are 2 directions of the same trend, namely directly proportional while 1 chart shows a negative trend direction or inversely. When the amount of silica oxide (Si-O) increases, the amount of iron oxide (Fe-O) decreases, and vice versa if the content of silica oxide (Si-O) increases, the amount of iron oxide (Fe-O) also increases.

X-Ray diffractometer (XRD)

The results of characterization with XRF showed that the sediment samples indicated the presence of magnetic properties. To find out exactly the type of mineral, characterization is carried out with X-Ray Diffraction (XRD). The results of the characterization obtained a diffraction pattern consisting of several peaks. By using the OriginLab software the results are plotted for the y-axis in the form of peak intensity and the x-axis from the measured diffraction angle. At each peak that is in a diffraction pattern formed because the X-ray beam is diffracted from the plane in the sample material. Therefore, each peak has a mutually proportional intensity and number of x-ray photons that can be detected by detectors at each angle.

In **Figures 5(a) - 5(c)** confirm the pattern of XRD characterization results from sediment samples in the upstream-downstream of the Bengawan Solo [48]. The comparison results of XRD characterization were assisted by the HighScore Plus application with data from COD (Crystallography Open Database). Old Lawu Mountain found several minerals including albite and cristobalite. The mineral cristobalite is silica which is formed from the final process of crystallization of volcanic rocks.

The mineral cristobalite (SiO_2) like the mineral quartz (SiO_2) is a mineral that is formed in the intermediate weathering stage. Magnetite minerals are also found on Mount Lawu. According to [49], ferromagnetic minerals one of which is magnetite is not affected by weathering because it has low coercivity. The XRD results from the upstream-downstream Bengawan Solo samples are presented in **Table 4**. The minerals contained in the Bengawan Solo River sample are very rich in minerals originating from various sources. These sources can come from Mount Lawu, Mount Merapi and even Mount Wilis.

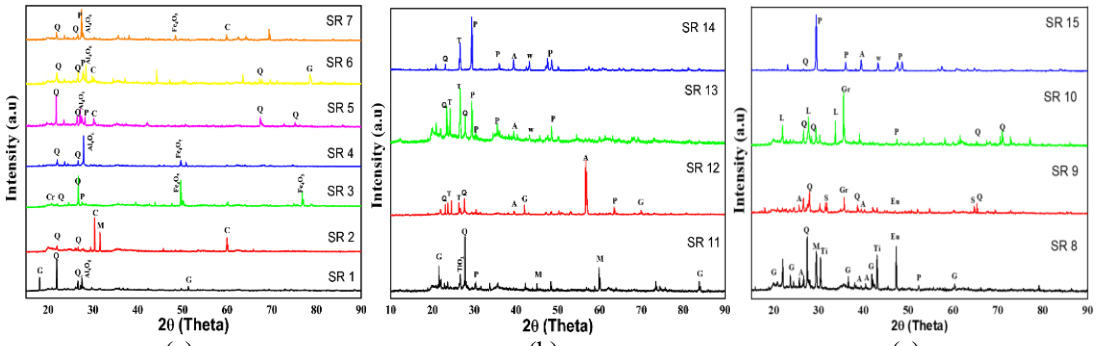

(a) (b) (c)

Figure 5 The diffraction pattern generated by the Bengawan Solo sample section; (a) upstream; (b) Middle; (c) Downstream.

Table 4 List of minerals contained in the upstream-downstream bengawan solo samples.

Symbol	Mineral	Compound	Description
C	Coesite	SiO_2	Formed when very high pressure, and high enough temperature, is applied to quartz [50].
M	Magnetite	Fe_3O_4	The mineral has the most magnetic properties among all the natural minerals on earth [51].

Symbol	Mineral	Compound	Description
Cr	Cristobalite	SiO_2	Formed at very high temperatures with moderate pressure [52].
P	Portlandite	$Ca(OH)_2$	A natural form of calcium hydroxide and a calcium analogue of brucite [53].
Q	Quartz	SiO_2	The second mineral we can found in earth behind feldspar
A	Anatase	TiO_2	Anatase in nature is usually a black solid because of impurities [54].
Ge	Goethite	$Fe_3O(OH)$	An oxide mineral that can be found in soil and low temperature environments [41].
T	Tridymite	SiO_2	White or colorless, or scales, in cavities in felsic volcanic rocks [55].
G	Gibbsite	$Al(OH)_3$	Important ore in aluminum mining, and is one of the compositions of bauxite rocks [56].
S	Stishovite	SiO_2	The extremely hard and dense tetragonal form of silicon dioxide
Gr	Grasullaria	$Ca_3Al_2(SiO_4)_3$	Calcium can be replaced by iron and aluminum [57].
L	Labradorite	$((Ca, Na)(Al, Si)_4O_8)$	A type of mineral feldspar
W	Wuestite	FeO	A natural Iron

In **Table 4**, the minerals contained in the sample are presented. Some minerals are included in iron oxide. Elemental iron oxide makes the sample contain magnetic properties. Coesite minerals are formed from high temperatures and pressures which are characteristic of volcanic eruptions. During a volcanic eruption, the high temperature inside the earth is very different compared to the temperature outside the earth. Similarly, the pressure temperature inside the bowels of the earth is much higher than outside the bowels of the earth.

Vibrating sample magnetometer (VSM)

VSM is an instrument used in determining the magnetic properties of Bengawan Solo sediments from upstream to downstream. The characterization value is defined as the yielding hysteresis curve Magnetization (M) and Magnetic Field (H) in **Figure 6**. In **Figures 6(a) - 6(c)** can see the magnetic properties of the material in different parts. In part (a) the hysteresis curve has a nearly symmetrical reverse sequence when subjected to a magnetic field or when the magnetic field is removed.

This is due to the very small amount of magnetic mineral content in the sample. Dominated by non-magnetic minerals. The hysteresis curves in **Figures 6(a) - 6(c)** have a narrow area which indicates the energy required for the magnetization process. So that **Figures 6(a) - 6(c)** shows S-type hysteresis curve the presence of ferromagnetic characteristics from the sediment [58].

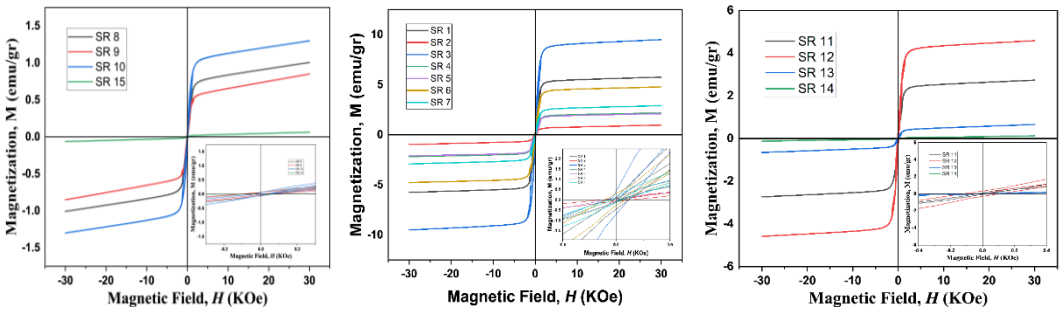

(a) (b) (c)

Figure 6 The magnetic properties of bengawan solo. We can see at; (a) Downstream Section, (b) Upstream Section, and (c) Middle part.

Magnetic susceptibility values can be plotted to obtain the magnetic properties of the rock. Using formula $\chi = dM/dH$, where χ is the magnetic susceptibility value, while M is the magnetization and H is the external magnetic field that is inserted into the sample. So, we can know the magnetic domains contained in the Bengawan Solo samples upstream-downstream. Look at **Figure 7** and **Table 5**. Based on **Table 5** the magnetic saturation values of all samples ranged from 0.06 - 9.4 (emu/gr) while the magnetic remanent were between 0.001 - 0.575 (emu/gr). Coercivity field values in the samples ranged from 10 - 60.15 (Oe). From the value of the coercivity field, the sample of Bengawan Solo River is classified as soft magnetic.

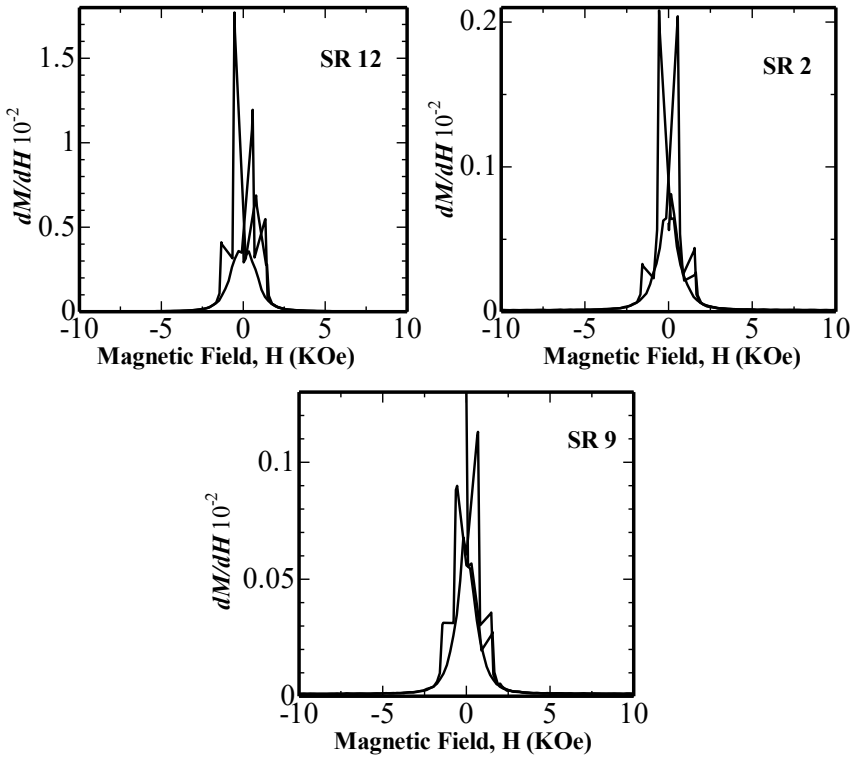

Figure 7 A partial snapshot of the sample in magnetic domain determination is contained in (a) Downstream sample (SR 12), (b) Upstream sample (SR 2), and (c) Middle sample (SR 9).

Table 5 Magnetic saturation (Ms), magnetic remanent, and magnetic coersivity.

Code	Ms (emu/gr)	Mr (emu/gr)	Mr/Ms	Hc (Oe)
SR 1	5.745	0.295	0.051	13.5
SR 2	1.023	0.076	0.074	70
SR 3	9.440	0.575	0.061	47
SR 4	2.190	0.110	0.050	18.5
SR 5	2.070	0.085	0.041	60.15
SR 6	4.750	0.289	0.061	40
SR 7	2.920	0.120	0.041	30
SR 8	1.000	0.050	0.050	30
SR 9	0.860	0.040	0.047	20
SR 10	1.300	0.047	0.036	15
SR 11	2.740	0.090	0.033	31
SR 12	4.590	0.320	0.070	60
SR 13	0.650	0.030	0.046	33.5
SR 14	0.120	0.001	0.009	29.5
SR 15	0.060	0.001	0.010	10

Based on **Table 5** the value of Mr/Ms presented is less than 0.05. According to [59-62], the value of Mr/Ms can be a factor for determining the magnetic domain of a sample. The results of Mr/Ms if the value is less than 0.5 can be entered into the multi-domain category, if the value is more than 0.5 it can be entered into the single-domain category. As seen in **Table 5** all samples fall into the multi-domain category and in **Figure 7** an overview of the multi-domains obtained from the plotting between the magnetic field values (H) and magnetic susceptibility values (*dM/dH*) is presented.

Conclusions

The magnetic properties of the lower and middle Bengawan Solo are affected by the eruption of ancient Mount Lawu. Eruption material is sedimented on the bottom and in the Bengawan Solo environment with a confirmed magnetic susceptibility value of around $1{,}080.23\times10^{-8}$ m^3/Kg - $2{,}780.77\times10^{-8}$ m^3/Kg, the middle part is 74.40×10^{-8} m^3/Kg - $1{,}735.90\times10^{-8}$ m^3/Kg, and downstream 17.57×10^{-8} m^3/Kg - $1{,}620.53\times10^{-8}$ m^3/Kg. From these results, there is a reduction in the magnetic value from downstream to upstream. Starting from the central part to the Upper Bengawan Solo, there is an eroding process caused by heavy water flow and imperfect sedimentation processes in the Bengawan Solo environment. Magnetic properties being ferromagnetic which can be seen clearly from the hysteresis curve formed. The curve that forms like the letter S (S-type) is the easiest to recognize. Assisted by the minerals contained, it is true that all samples are ferromagnetic. Mr/Ms value of less than 0.5 indicated of multi-domain. All samples have a magnetic susceptibility value that must be supported by metal oxide. Dominated by Fe-O, Si-O, and Al-O. So that the Bengawan Solo River is rich in minerals sourced from Iron oxide. X-Ray Diffractometer confirmed the minerals contained in the sample were Coesite, Magnetite, Cristobalite, Portlandite, Quartz, Anatase, Goethite, Tridymite, Gibsyte, Stishovite, Grasullaria, Labradorite and Wuestite. The minerals obtained indicate that Bengawan Solo is the result of an eruption from a volcano.

Acknowledgements

This research was funded by the DIPA of Universitas Sebelas Maret of The Republic 286 of Indonesia (Hibah PDD PNBP Kontrak No. 260/UN27.22/HK.07.00/2021).

References

[1] MF Hannum, IP Santikayasa and M Taufik. The use of dam environmental vulnerability index (DEVI) for assessing vulnerability of Bengawan Solo Watershed, Indonesia. *Agromet* 2020; **34**, 110-20.

[2] BG Koffman, MF Yoder, T Methven, L Hanschka, HB Sears, PL Saylor and KL Wallace. Glacial dust surpasses both volcanic ash and desert dust in its iron fertilization potential. *Global Biogeochem. Cy.* 2021; **35**, e2020GB006821.

[3] M Mariyanto, MF Amir, W Utama, AM Hamdan, S Bijaksana, A Pratama, R Yunginger and S Sudarningsih. Heavy metal contents and magnetic properties of surface sediments in volcanic and tropical environment from Brantas River, Jawa Timur Province, Indonesia. *Sci. Total Environ.* 2019; **675**, 632-41.

[4] W Zhuo, B Lei, S Wu, F Yu, C Zhu, J Cui, Z Sun, D Ma, M Shi, H Wang, W Wang, T Wu, J Ying, S Wu, Z Wang, and X Chen. Manipulating ferromagnetism in few-layered $Cr_2Ge_2Te_6$. *Adv. Mater.* 2021; **33**, 2008586.

[5] T Yin, KA Ulman, S Liu, AGd Águila, Y Huang, L Zhang, M Serra, D Sedmidubsky, Z Sofer, SY Quek, and Q Xiong. Chiral phonons and giant magneto-optical effect in $CrBr_3$ 2D magnet. *Adv. Mater.* 2021; **33**, 2101618.

[6] S Mugiraneza and AM Hallas. Tutorial: A beginner's guide to interpreting magnetic susceptibility data with the curie-weiss law. *Comm. Phys.* 2022; **5**, 95.

[7] NP Prasetya, Utari, Y Iriani and B Purnama. The effect of annealing temperature on the structural and magnetic properties of lanthanum doped cobalt ferrite with the bengawan solo river fine sediment as the source of Fe3+. *Key Eng. Mater.* 2023; **940**, 11-20.

[8] Mariyanto and S Bijaksana. Magnetic properties of surabaya river sediments, East Java, Indonesia. *AIP Conf. Proc.* 2017; **1861**, 030045.

[9] A Juliansyah, S Zulaikah, N Mufti, EY Agustin, R Pujiastuti and BH Iswanto. Magnetic susceptibility of river sediment in polluted area of traditional gold mining in Kuris Sumbawa Indonesia. *AIP Conf. Proc.* 2020; **2251**, 040020.

[10] M Li, S Zhu, T Ouyang, J Tang and Z Tang. Magnetic properties of the surface sediments in the Yellow River Estuary and Laizhou Bay, Bohai Sea, China: Implications for monitoring heavy metals. *J. Hazard. Mater.* 2021; **410**, 124579.
[11] J Huang, W Jiao, J Liu, S Wan, Z Xiong, J Zhang, Z Yang, A Li , and T Li. Sediment distribution and dispersal in the southern South China Sea: Evidence from clay minerals and magnetic properties. *Mar. Geol.* 2021; **439**, 106560.
[12] J Yang, D Xia, Z Chen, S Wang, F Gao, X Liu, S Zhao, L Zhao, and Y Liu. Differentiating detrital and pedogenic contributions to the magnetic properties of aeolian deposits in the southern Tibetan Plateau: Implications for paleoclimatic reconstruction. *Catena*, 2023; **220**, 106736.
[13] F Wang, W Zhang, T Huang, Y Xu and Z Lai. Particle-size dependent magnetic property variations in the Yangtze delta sediments of late Holocene: Effects of pedogenesis and diagenesis. *CATENA* 2022; **209**, 105832.
[14] H Moulouel, A Bouchelouh, R Bensalem, MY Tebbouche, DA Benamar, EH Oubaiche, S Gharbi, D Machane, and A Benamghar. The Mahelma fault: A secondary structure of the Sahel anticline? *Arabian J. Geosci.* 2020; **13**, 715.
[15] M Roma, O Vidal-Royo, K McClay, O Ferrer and JA Muñoz. Tectonic inversion of salt-detached ramp-syncline basins as illustrated by analog modeling and kinematic restoration. *Interpretation* 2018; **6**, T127-44.
[16] S He, Q Qin, H Li and S Wang. Deformation differences in complex structural areas in the Southern Sichuan Basin and its influence on shale gas preservation: A case study of Changning and Luzhou areas. *Front. Earth Sci.* 2022; **9**, 818534.
[17] DC Tanner, H Buness, J Igela, T Gunther, G Gabriel, P Skiba, T Plenefisch, N Gestermann, and TR Walter. Fault detection. *Understand. Faults* 2020; **2020**, 81-146.
[18] Y Wang, ME Oskin, H Zhang, Y Li, X Hu and J Lei. Deducing crustal-scale reverse-fault geometry and slip distribution from folded river terraces, Qilian Shan, China. *Tectonics* 2020; **39**, e2019TC005901.
[19] JCA Joordens, FP Wesselingh, JD Vos, HB Vonhof and D Kroon. Relevance of aquatic environments for hominins: A case study from Trinil (Java, Indonesia). *J. Hum. Evol.* 2009; **57**, 656-71.
[20] W Joordens, JC D'Errico, F Wesselingh, FP Munro, SD Vos, J Wallinga, F d'Errico, FP Wesselingh, S Munro, JD Vos, J Wallinga, C Ankjærgaard, T Reimann, JR Wijbrans, KF Kuiper, HJ Mücher, H Coqueugniot, V Prié, I Joosten, BV Os, AS Schulp, M Panuel, VVD Haas, W Lustenhouwer, JJG Reijmer and W Roebroeks. Homo erectus at Trinil on Java used shells for tool production and engraving. *Nature* 2015; **518**, 228-31.
[21] G Alink, W Roebroeks and T Simanjuntak. The Homo erectus site of Trinil: Past, present and future of a historic place. *AMERTA* 2016; **34**, 99.
[22] JC Hilgen, E Pop, S Adhityatama, TA Veldkamp, HWK Berghuis, I Sutisna, D Yurnaldi, GD Nivet, T Reimann, N Nowaczyk, KF Kuiper, W Krijgsman, HB Vonhof, DR Ekowati, G Alink, NLGDM Hafsari, O Drespriputra, A Verpoorte, R Bos, T Simanjuntak, B Prasetyo, and JCA Joordens. Revised age and stratigraphy of the classic Homo erectus-bearing succession at Trinil (Java, Indonesia). *Quaternary Sci. Rev.* 2023; **301**, 107908.
[23] E Venzke. *Global volcanism program*. Volcanoes of the World. Smithsonian Institution, Washington D.C., 2022. https://doi.org/10.5479/si.GVP.VOTW5-2022.5.0
[24] GI Marliyani, H Helmi, JR Arrowsmith and A Clarke. Volcano morphology as an indicator of stress orientation in the Java Volcanic Arc, Indonesia. *J. Volcanol. Geoth. Res.* 2020; **400**, 106912.
[25] V Memoli, E Eymar, CG Delgado, F Esposito, L Santorufo, AD Marco, R Barile, and G Maisto. Total and fraction content of elements in volcanic soil: Natural or anthropogenic derivation. *Sci. Total Environ.* 2018; **625**, 16-26.
[26] DD Lestiani, R Apryani, L Lestari, M Santoso, EP Hadisantoso and S Kurniawati. Characteristics of trace elements in volcanic ash of kelud eruption in East Java, Indonesia. *Indonesian J. Chem.* 2018; **18**, 457-63.
[27] Q Ma, L Han, J Zhang, Y Zhang, Q Lang, F Li, A Han, Y Bao, K Li and S Alu. Environmental risk assessment of metals in the volcanic soil of Changbai mountain. *Int. J. Environ. Res. Publ. Health* 2019; **16**, 2047.
[28] M Liotta, MM Cruz, A Ferrufino, J Rüdiger, A Gutmann, KVR Cerda, N Bobrowski, and JMD Moor. Magmatic signature in acid rain at Masaya volcano, Nicaragua: Inferences on element volatility during lava lake degassing. *Chem. Geol.* 2021; **585**, 120562.
[29] RN Fajri, R Putra, CBD Maisonneuve, A Fauzi, Yohandri and H Rifai. Analysis of magnetic properties rocks and soils around the Danau Diatas, West Sumatra. *J. Phys. Conf.* 2019; **1185**, 012024.

[30] E Venzke. *Global volcanism program*. Volcanoes of the World. Smithsonian Institution, Washington D.C., 2023. https://doi.org/10.5479/si.GVP.VOTW5-2022.5.0
[31] A Sasmita, H Rifai, R Putra, N Aisyah, M Phua, S Eisele, F Forni, and CBDL Maisonneuve. Identification of magnetic minerals in the peatlands cores from Lake Diatas West Sumatra, Indonesia. *J. Phys. Conf.* 2020; **1481**, 012019.
[32] R Padawangi, P Rabé and A Perkasa. *River cities in asia: Water space in urban development and history*. Amsterdam University Press B.V., Amsterdam, Netherlands, 2022.
[33] S Matsu'ura, M Kondo, T Danhara, S Sakata, H Iwano, T Hirata, I Kurniawan, E Setiyabudi, Y Takeshita, M Hyodo, I Kitaba, M Sudo, Y Danhara, and Fachroel Aziz. Age control of the first appearance datum for Javanese Homo erectus in the Sangiran area. *Science* 2020; **367**, 210-4.
[34] W Mwandira, K Nakashima and S Kawasaki. Bioremediation of lead-contaminated mine waste by Pararhodobacter sp. based on the microbially induced calcium carbonate precipitation technique and its effects on strength of coarse and fine grained sand. *Ecol. Eng.* 2017; **109**, 57-64.
[35] S Indiketiya, P Jegatheesan, P Rajeev and R Kuwano. The influence of pipe embedment material on sinkhole formation due to erosion around defective sewers. *Transport. Geotechnics* 2019; **19**, 110-25.
[36] R Tyszka, A Pietranik, A Potysz, J Kierczak and B Schulz. Experimental simulations of Zn-Pb slag weathering and its impact on the environment: Effects of acid rain, soil solution, and microbial activity. *J. Geochem. Explor.* 2021; **228**, 106808.
[37] C Zhao, D Mo, J Yuxiang, P Lu, L Bin, N Wang, M Chen, Y Liao, P Zhan, and Y Zhuang. A 7000-year record of environmental change: Evolution of holocene environment and human activities in the Hangjiahu Plain, the lower Yangtze, China. *Geoarchaeology* 2022, https://doi.org/10.1002/gea.21945.
[38] H Mosaid, A Barakat, V Bustillo and J Rais. Modeling and mapping of soil water erosion risks in the Srou Basin (Middle Atlas, Morocco) using the EPM model, GIS and magnetic susceptibility. *J. Landsc. Ecol.* 2022; **15**, 126-47.
[39] VA Tiwow, Subaer, Sulistiawaty, JD Malago, MJ Rampe and M Lapa. Magnetic susceptibility of surface sediment in the Tallo tributary of Makassar city. *J. Phys. Conf.* 2021; **1899**, 012124.
[40] A Rahmi, H Rifai, R Rahmayuni, AN Yuwanda, DA Visgun and L Dwiridal. Irregular magnetic susceptibility pattern of iron sand from pasia jambak beach, Pasia Nan Tigo, Padang, Indonesia. *J. Phys. Conf.* 2022; **2309**, 012027.
[41] X Zhao, W Zhang, F Wang, QL Vu and Y Saito. Late Holocene sediment provenance change in the Red River Delta: A magnetic study, Catena. *Catena* 2023; **220**, 106685.
[42] S Putra, H Rifai, R Fadila, ED Ningsih and R Putra. Distribution of Pyroclastic deposits around Lake Maninjau Agam District, West Sumatera, Indonesia based on Magnetic Susceptibility. *Trends Sci.* 2022; **19**, 3218.
[43] F Laha, F Gashi, S Frančišković-Bilinski, H Bilinski and H Çadraku. Geospatial distribution of heavy metals in sediments of water sources in the Drini i Bardhë river basin (Kosovo) using XRF technique. *Sustain. Water Resour. Manag.* 2022; **8**, 31.
[44] G Jha, S Mukhopadhyay, AL Ulery, K Lombard, S Chakraborty, DC Weindorf, D VanLeeuwen and C Brungard. Agricultural soils of the animas river watershed after the gold king mine spill: An elemental spatiotemporal analysis via portable x-ray fluorescence spectroscopy. *J. Environ. Qual.* 2021; **50**, 730-43.
[45] F Riminucci, V Funari, M Ravaioli and L Capotondi. Trace metals accumulation on modern sediments from Po river prodelta, North Adriatic Sea. *Mar. Pollut. Bull.* 2022; **175**, 113399.
[46] L Wu, M Peng, S Qiao and M Xiao-yi. Effects of rainfall intensity and slope gradient on runoff and sediment yield characteristics of bare loess soil. *Environ. Sci. Pollut. Res.* 2018; **25**, 3480-7.
[47] VR Troll, FA Weis, E Jonsson, UB Andersson, SA Majidi, K Högdahl, C Harris, MA Millet, SS Chinnasamy, E Kooijman and KP Nilsson. Global Fe-O isotope correlation reveals magmatic origin of Kiruna-type apatite-iron-oxide ores. *Nat. Comm.* 2019; **10**, 1712.
[48] B Legowo, R Nailatunisrina, H Purwanto, B Purnama, and W Suryanto. Modelling of Volcano Lawu Fault Structure Using Gravity Anomaly to Determine Landslides Potential. IOP Conference Series: Earth and Environmental Science. 2022, p. **012025**.
[49] DP Maxba.uer, JM Feinberg, DL Fox and WC Clyde. Magnetic minerals as recorders of weathering, diagenesis, and paleoclimate: A core-outcrop comparison of Paleocene-Eocene paleosols in the Bighorn Basin, WY, USA. *Earth Planet. Sci. Lett.* 2016; **452**, 15-26.
[50] TN Chen, Ren-Xu Chen, Yong-Fei Zheng, Kun Zhou, Zhuang-Zhuang Yin, Zhi-Min Wang, Bing Gong, and Xiang-Ping Zha. The effect of supercritical fluids on Nb-Ta fractionation in subduction

zones: Geochemical insights from a coesite-bearing eclogite-vein system. *Geochim. Cosmochim. Acta* 2022; **335**, 23-55.

[51] AG Niculescu, C Chircov and AM Grumezescu. Magnetite nanoparticles: Synthesis methods - a comparative review. *Methods* 2021; **199**, 16-27.

[52] Z Yan, W Xue and D Mei. Density functional theory study on the morphology evolution of hydroxylated β-Cristobalite silica and desilication in the presence of methanol. *J. Phys. Chem. C* 2021; **125**, 7868-79.

[53] D Approach, K Mohammad, S Uddin, M Izadifar and N Ukrainczyk. Dissolution of portlandite in pure water : Part 1 molecular. *Materials* 2022; **15**, 1404.

[54] S Liang, X Wang, C Ya-Jun, Y Xia and P Müller-Buschbaum. Anatase titanium dioxide as rechargeable ion battery electrode - a chronological review. *Energ. Storage Mater.* 2022; **45**, 201-64.

[55] V Payré, KL Siebach, MT Thorpe, P Antoshechkina and EB Rampe. Tridymite in a lacustrine mudstone in Gale Crater, Mars: Evidence for an explosive silicic eruption during the Hesperian. *Earth Planet. Sci. Lett.* 2022; **594**, 117694.

[56] A Klaassen, F Liu, F Mugele and I Siretanu. Correlation between electrostatic and hydration forces on silica and gibbsite surfaces: An atomic force microscopy study. *Langmuir* 2022; **38**, 914-26.

[57] M Gaft, G Waychunas, GR Rossman, L Nagli, A Goryachev and Y Raichlin. Zero-phonon Mn^{2+} luminescence in natural grossular $Ca_3Al_2(SiO_4)_3$. *J. Lumin.* 2022; **248**, 119001.

[58] JD Winter. *An introduction to igneous and metamorphic petrology*. Pearson College Div, London, 2001.

[59] N Boda, Gopal Boda, K. Chandra Babu Naidu, M. Srinivas, Khalid Mujasam Batoo, D. Ravinder, and A. Panasa Reddy. Effect of rare earth elements on low temperature magnetic properties of Ni and Co-ferrite nanoparticles. *J. Magn. Magn. Mater.* 2019; **473**, 228-35.

[60] N Raghuram, TS Rao and KCB Naidu. Magnetic properties of hydrothermally synthesized $Ba_{1-x}Sr_xFe_{12}O_{19}$ (x = 0.0–0.8) nanomaterials. *Appl. Phys. Mater. Sci. Process.* 2019; **125**, 839.

[61] A Gaffoor, KCB Naidu, D Ravinder, KM Batoo, SF Adil and M Khan. Synthesis of nano-$NiXFe_2O_4$ (X = Mg/Co) by citrate-gel method: Structural, morphological and low-temperature magnetic properties. *Appl. Phys. Mater. Sci. Process.* 2020; **126**, 39.

[62] TV Sagar, TS Rao and KCB Naidu. Effect of calcination temperature on optical, magnetic and dielectric properties of Sol-Gel synthesized $Ni_{0.2}Mg_{0.8-x}Zn_xFe_2O_4$ (x = 0.0–0.8). *Ceram. Int.* 2020; **46**, 11515-29.